Indian Journal of Pure & Applied Physics
Vol. 56, March 2018, pp. 196-202

# An ultrathin polarization insensitive frequency selective surface for wide stop band RF applications

S Garg, D Sood* & K Gopal

Department of Electronics and Communication Engineering, University Institute of Engineering & Technology, Kurukshetra University, Kurukshetra 136 119, India

*Received 19 May 2017; accepted 20 October 2017*

In this paper, a compact, polarization insensitive, wide stop band frequency selective surface (FSS) has been proposed to serve C, X and Ku band applications. The unit cell of the proposed FSS consists of the combination of square loop and Jerusalem cross dipole elements to achieve wide stop band with a -10 dB bandwidth of 15.96 GHz from 5.45 GHz to 21.41 GHz. The periodicity and overall thickness of the structure are 0.32 $\lambda_0$ and 0.04 $\lambda_0$, respectively. The proposed design is polarization insensitive and provides a wide stop band response for large angles of incident wave with TE or TM polarization. Equivalent circuit analysis has also been performed to verify the simulated results. A prototype of proposed structure has been fabricated and experimentally tested. The measured results have been observed in agreement with the simulated results.

**Keywords**: Frequency selective surface, Spatial filter, Polarization insensitive, Wideband FSS

## 1 Introduction

Frequency selective surfaces (FSSs) are periodic structures consisting of an assembly of conducting elements arranged in one or two dimensional array[1]. These were originally developed for electromagnetic filtering, i.e., selective transmission, reflection and absorption of an incident wave[2]. FSSs have a range of applications such as meander line polarizer[3], band pass radome to efficiently reduce the radar cross section (RCS) of an antenna[4], sub reflector for dual frequency reflector system[5], electromagnetic absorbers[6-7], beam splitters[8] and optical filters[9], etc. The frequency response of a FSS structure can be controlled by optimizing different parameters such as periodicity of unit cell, element type, inter-element spacing and substrate thickness. A wideband FSS can be designed by using multilayer structures[10], thicker substrate[11] and optimizing inter-element spacing[1]. Different wideband FSS design configurations have been investigated in the literature[12-17]. The FSS structure proposed by Sivasamy *et al.*[12] is polarization insensitive wideband FSS but its unit cell size and thickness is still large. The design reported by Chatterjee and Parui[13] provides wideband response, but its multilayer configuration limits its applications. The FSS proposed by Kushwaha *et al.*[14] exhibits ultra-wideband response, but its polarization sensitive design limits its practical use. The FSSs reported by Braz and Campos[15] and Sohail *et al.*[16] have larger unit cell size and thickness. The FSS structure presented by Yahya *et al.*[17] provides large bandwidth with smaller unit cell size and thickness but it covers only C and X band.

In this paper a compact polarization insensitive band stop FSS has been presented for wide band RF applications. The proposed design exhibits the -10 dB bandwidth of 15.96 GHz. The unit cell dimension of the proposed design is 7.24 × 7.24 mm$^2$, i.e., 0.32 $\lambda_0$ × 0.32 $\lambda_0$ ($\lambda_0$ is the operating wavelength corresponding to the center frequency of -10dB bandwidth). The proposed FSS design is compact and ultra-thin. The design is made four fold symmetric to achieve insensitivity for all angles of polarization under normal incidence of electromagnetic wave. The equivalent circuit model for square loop and Jerusalem cross has been analyzed and circuital parameters are determined.

## 2 Unit Cell Design

The type of FSS element is chosen based on specific requirements such as operating bandwidth and frequency response, stability for wide incident angles under different polarization conditions. For the proposed design, in order to achieve wideband two different FSS elements are combined. The dimensions of individual elements are optimized in such a way that they exhibit transmission nulls at different frequencies. The unit cell design with optimized dimensions is

*Corresponding author (E-mail: deepaksood.uiet@gmail.com)

shown in Fig. 1. The metallic layer at the top surface is designed with the combination of square loop and Jerusalem cross elements printed on 1 mm thick un-grounded FR-4 dielectric substrate ($\varepsilon_r = 4.4$ and $\tan\delta = 0.02$). The overall thickness of the designed structure is around $0.043\lambda_0$. The design is periodic with the periodicity of 7.24 mm which is $0.32\ \lambda_0$ in both the X and Y directions.

## 3 Simulation

The simulation of the proposed FSS is carried through the use of HFSS simulation tool by applying Floquet's periodic boundary conditions. The transmission response under normal incidence of the electromagnetic wave is shown in Fig. 2. It is observed that the proposed structure exhibits a -10 dB bandwidth of 15.96 GHz from 5.45 GHz to 21.41 GHz.

The structure is also analyzed for different angles of polarization ($\phi$) under normal incidence as shown in Fig. 3. It is noticed that the transmission response remains same for all polarization angles which verifies that the proposed design is polarization insensitive. The proposed FSS design is also examined for different oblique angles of the incident wave with TE and TM polarizations as shown in Figs 4 and 5, respectively. It is observed that for both the polarizations as the

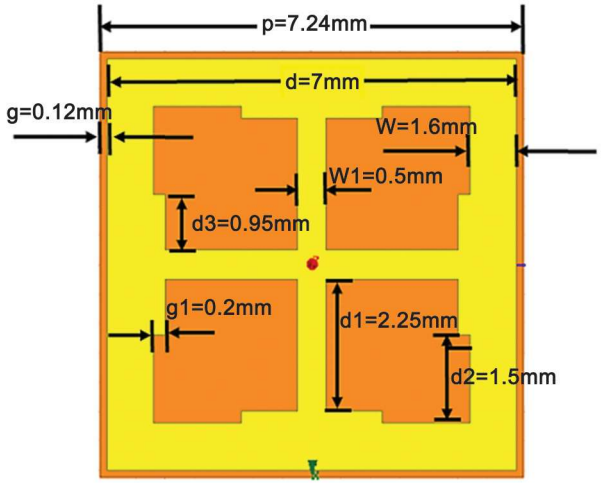


Fig. 1 — The unit cell design with optimized dimensions.

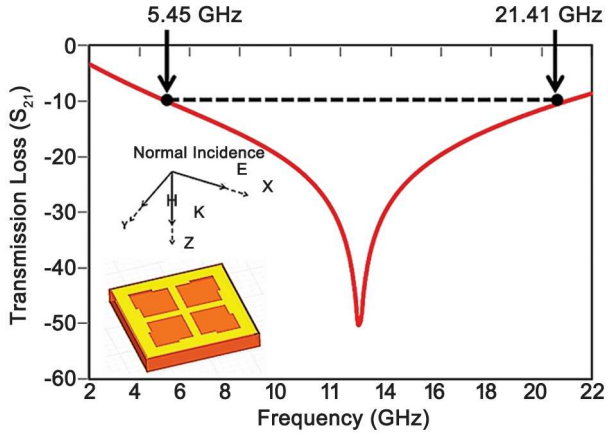


Fig. 2 — Transmission response under normal incidence of the electromagnetic wave.

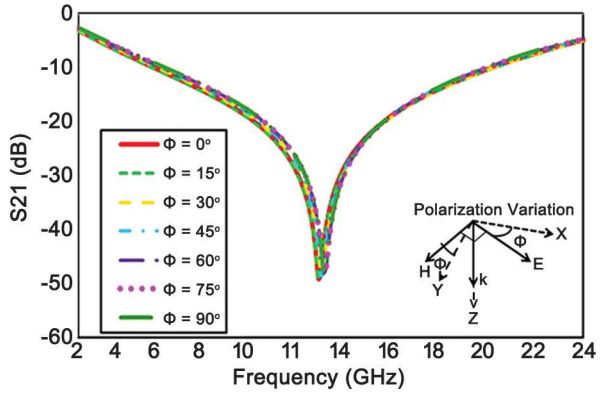


Fig. 3 — Simulated response for different angles of polarization (φ) under normal incidence.

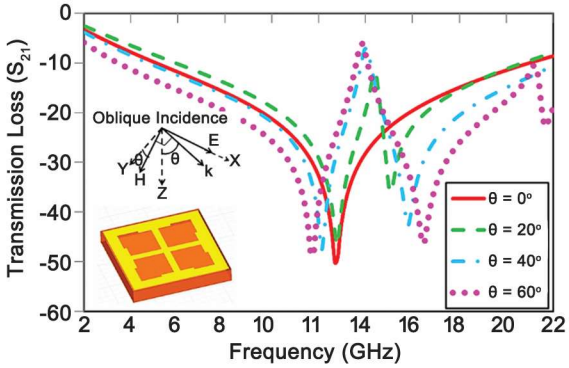


Fig. 4 — Simulated response for different oblique angles of the incident wave for TE polarization.

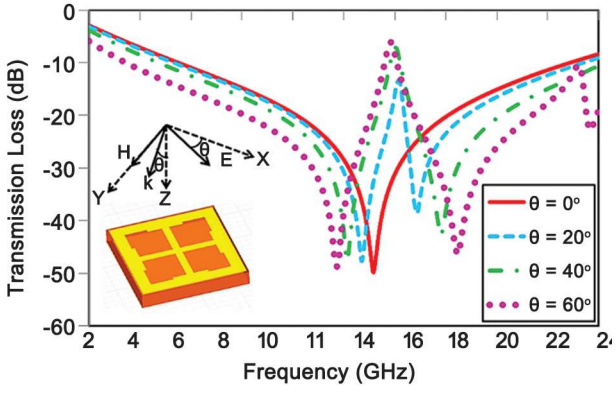


Fig. 5 — Simulated response for different oblique angles of the incident wave for TM polarization.

incident angle increases from 0° to 60° the wideband transmission response gradually changes to dual stop band and one pass band response. This happens due to the fact that with the increase in incident angle from 0° to 60° the coupling of incident electromagnetic field with the FSS structure changes. For the incident angle of 60°, the two transmission nulls are observed at frequencies of 11.78 and 16.49 GHz and one pass band peak is observed at 13.85 GHz. In order to investigate the variation of field coupling with the increase in incidence angle the electric and magnetic vector fields have been studied for 13.85 GHz at the incident angles of 0° to 60° as shown in Fig. 6. It is noticed that the effect of electric field almost remains similar with the increase in incident angle of the incoming wave as shown in Fig. 6(a, b). Further, as the incident angle increases to 60° the difference in distribution of magnetic field in proposed FSS design for 0° to 60° is clearly noticeable as shown in Fig. 6(c, d). Therefore, these variations of magnetic field coupling with the proposed FSS design are mainly responsible for the occurrence of pass band at 13.85 GHz thereby results dual stop band response with transmission null at 11.78 and 16.49 GHz.

## 4 Results and Discussion

### 4.1 Equivalent circuit analysis

The equivalent circuit concepts can be effectively used for designing the complicated electronics devices for microwave to optical frequency regime[18]. Therefore, in order to better understand the principle of operation of proposed FSS and to investigate the bandwidth enhancement by the use of combination of two different FSS elements, the equivalent circuits of square loop and Jerusalem cross have been separately analyzed.

At first the equivalent circuit of the square loop element has been analyzed as shown in Fig. 7(a). The square loop as shown in Fig. 7(b) is modeled by a

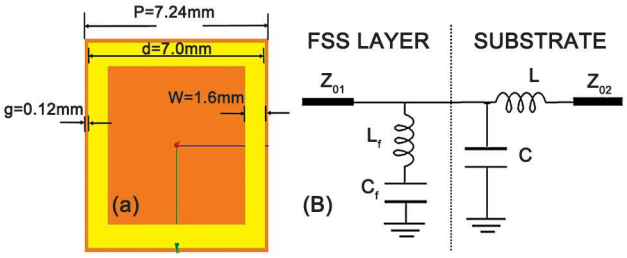


Fig. 7 — (a) Square loop element and its (b) equivalent circuit.

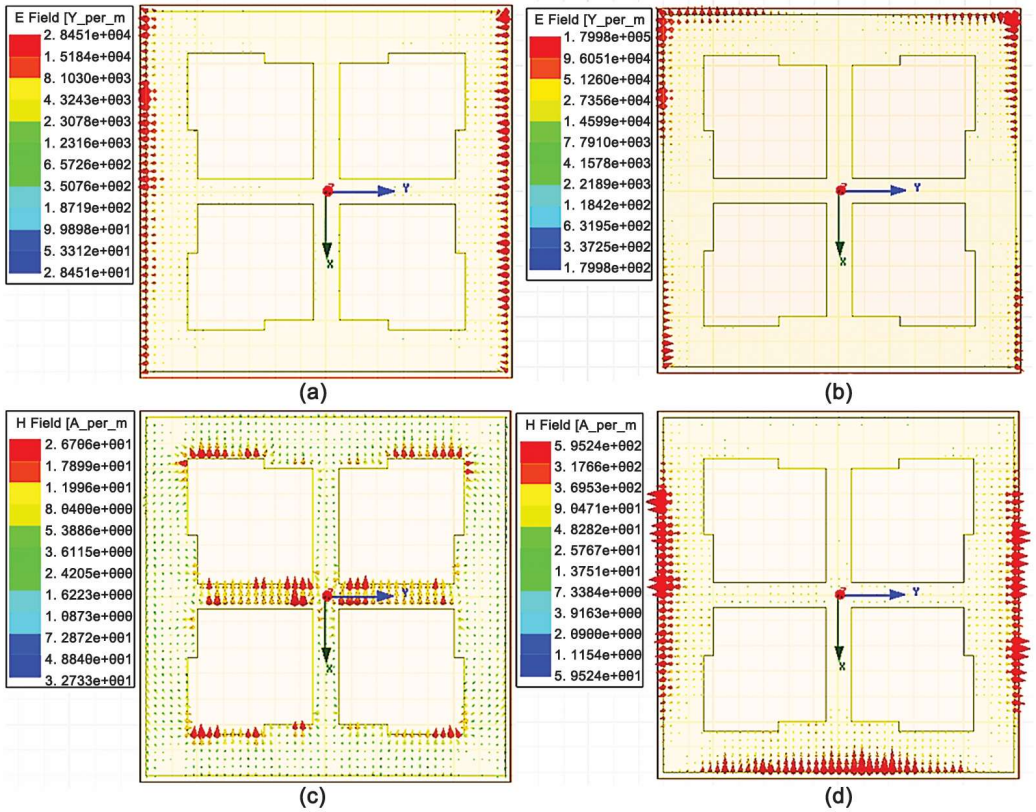


Fig. 6 — E-field vector at 13.85 GHz for (a) θ = 0° and (b) θ = 60° and H–field vector at 13.85 GHz for (c) θ = 0° and (d) θ = 60°.

resonant circuit in which $L_f$ and $C_f$ are connected in series in the shunt branch of the circuit and the dielectric substrate is modeled by the combination of $L$ in series and $C$ in a shunt branch of the circuit. The values of $L_f$ and $C_f$ are calculated as 1.57 nH and 0.12 pF, respectively, as per the relations given by Langley and Parker[19]. The values of $L$ and $C$ for the dielectric substrate are calculated as 1.27 nH and 0.95 pF, respectively, by using the relations as suggested by Al-Joumayly and Behdad[20]. The transmission null frequency is evaluated as 8.05 GHz. The simulated response of the square loop FSS element is shown in Fig. 8. The simulated transmission null is observed at 7.9 GHz, which is very close to the calculated value with a percentage error of only 1.86%. Thereafter, the equivalent circuit of the Jerusalem cross has been analyzed. Jerusalem cross with optimized dimensions is represented in Fig. 9(a) and it is modeled by the equivalent circuit[21] as shown in Fig. 9(b).

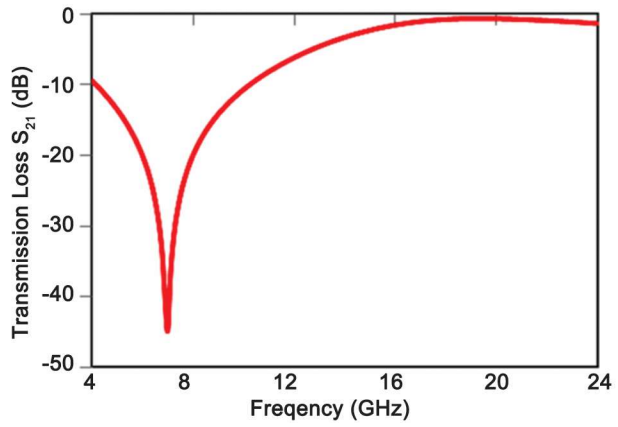


Fig. 8 — Simulated response of the square loop FSS element.

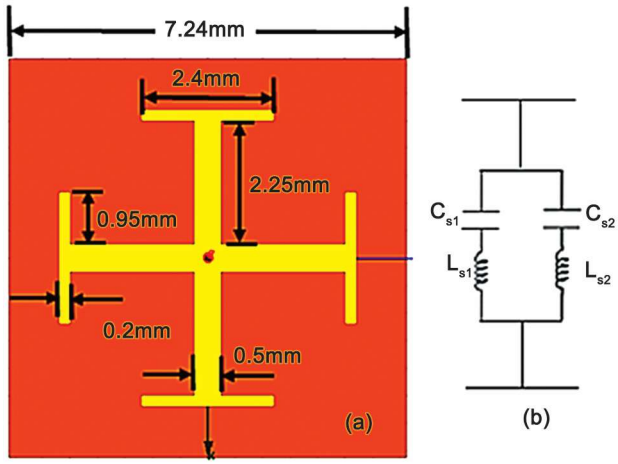


Fig. 9 — (a) Jerusalem cross type FSS element and its (b) equivalent circuit.

The calculated value of $L_{s1} = L_{s2}$ is 6.993 nH and of $C_{s1} = C_{s2}$ is 0.00735 pF. The calculated value of the frequency of the transmission null for the Jerusalem cross is 12.5 GHz. The simulated response of the Jerusalem cross is shown in Fig. 10.

The simulated frequency of transmission null is 12.7 GHz, which is almost equal to the calculated value. The simulated response of the two FSS elements (JCS and Square Loop) is compared in Fig. 11. It is observed from the simulated results and from the equivalent circuit analysis that the dimensions of both the FSS elements are optimized in such a way that they exhibit transmission nulls at different frequencies. Thus the combination of these two elements in a single unit cell (as in the proposed design) provides enhancement in bandwidth.

### 4.2 Wide stop band analysis

In order to achieve wide stop band and polarization insensitivity for the proposed FSS, a four stage process has been followed. In the first step, a square loop type

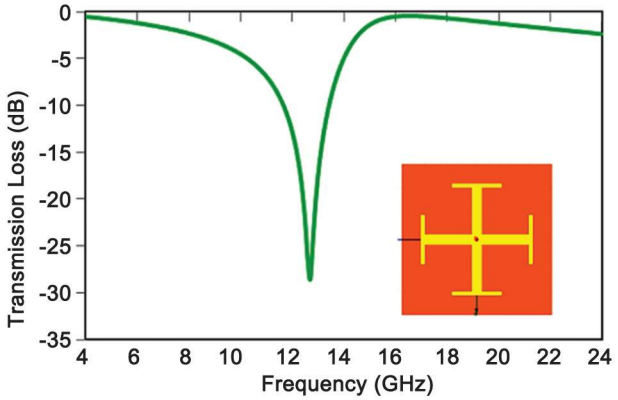


Fig. 10 — Simulated response of the Jerusalem cross type FSS element.

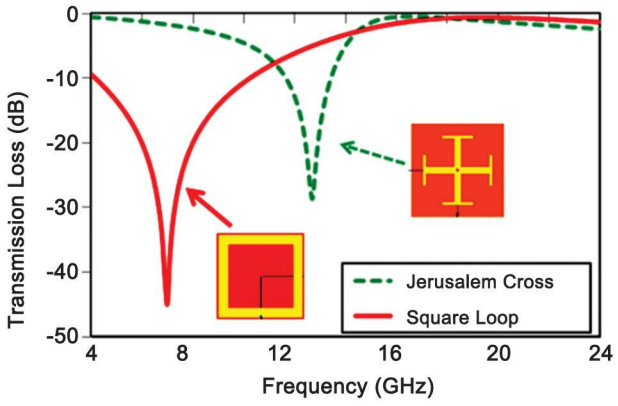


Fig. 11 — Comparison of simulation results of square loop and Jerusalem cross type FSS elements.

FSS element is chosen as a basic element to design a wideband FSS structure[2]. The simulated transmission response of the square loop element with optimized dimensions is shown in Fig. 12 as stage 1. It is observed that in stage 1 square loop FSS exhibits stop band with a -10 dB bandwidth of 6.06 GHz from 4.19 GHz to 10.25 GHz, with respect to the transmission null at a frequency of 7.04 GHz. Keeping in view that the combination of different FSS elements with closer resonating frequencies can provide wideband response, a cross dipole is used in combination with the square loop element in stage 2. The simulated transmission response for stage 2 is shown in Fig. 12. It is observed that in the stage 2, FSS exhibits a stop band with a -10 dB bandwidth of 14.87 GHz from 5.09 GHz to 19.96 GHz, with respect to the transmission null at a frequency of 12.05 GHz. Thereafter, in stage 3 end loadings are added in the cross dipole in order to increase the electrical length of the combined element. The addition of end loading converts the cross dipole into Jerusalem cross element[2] and increases the electrical length thereby broad bandwidth is achieved. The simulated transmission response for stage 3 design is shown in Fig. 12. It is observed that the FSS structure in stage 3 exhibits a stop band with a -10 dB bandwidth of 15.83 GHz from 4.99 GHz to 20.82 GHz, with respect to the transmission null at a frequency of 12.55 GHz. This stage provides wideband but to examine the effects of end loadings and to achieve the control of transmission null stage 4 is studied. In stage 4, the design of stage 3 has been modified by increasing the length of the end loadings in order to control the position of transmission null.

From the simulated response of stage 4 as shown in Fig. 12, it is observed that the FSS exhibits a wide stop band with a -10 dB bandwidth of 15.96 GHz from 5.45 GHz to 21.41 GHz, with the transmission null at a frequency of 13.27 GHz. As in stage 4 some increase in bandwidth as compared to stage 3 is observed therefore stage 4 is considered as final optimized FSS design. It is observed that as the design changes from the stage 1 to stage 4 the bandwidth gets increased from 6.06 GHz to 15.96 GHz corresponding to transmission null from 7.04 GHz to 13.27 GHz. Thus, in this way the two different FSS elements are combined with overall unit cell size of 0.32 $\lambda_0$ and thickness is 0.043 $\lambda_0$ corresponding to mean frequency (13.43 GHz) of the stop band. Therefore, it is concluded that the proposed design is compact and ultrathin. A comparison of bandwidth and transmission null frequencies for different design stages, i.e., 1 to 4 is given in Table 1.

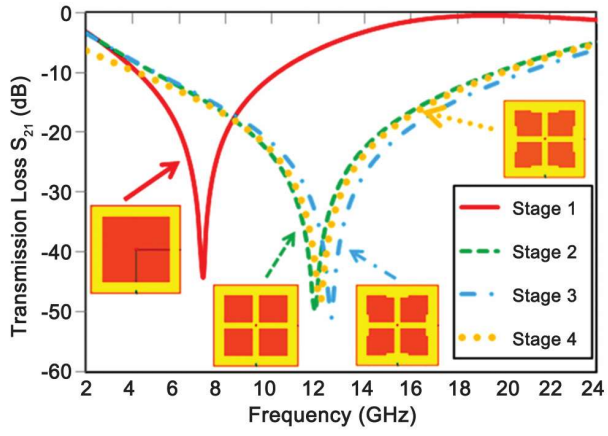


Fig. 12 — Comparison of simulation results from different design stages.

## 5 Fabrication and Measurements

A prototype array of the proposed FSS with 41×41 unit cells (30×30) cm$^2$ has been fabricated on a 1.0 mm thick FR4 dielectric substrate as shown in Fig. 13. Experimental verification of proposed FSS has been performed with the measurement setup shown in Fig. 14. Two double ridge UWB horn antennas with operating range 1 to 18 GHz connected to a vector analyzer (N5222A) have been used. The measurement

Table 1 — Comparison of different design stages.

| Design stages | Frequencies at transmission null (GHz) | Bandwidth (GHz) |
|---|---|---|
| 1 | 7.04 | 6.06 |
| 2 | 12.05 | 14.87 |
| 3 | 12.55 | 14.87 |
| 4 | 13.27 | 15.96 |

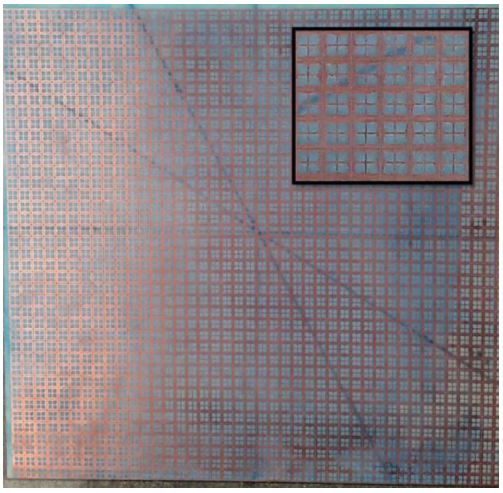

Fig. 13 — Fabricated prototype array of the proposed FSS.

is performed in two steps. At first, in order to calibrate the test environment the transmitted power in between the transmitting and receiving horn antennas has been measured. Thereafter, in the second step the transmitted power is measured, by placing the fabricated prototype FSS sample in between the two horn antennas. The actual transmission from the fabricated design is then evaluated by taking the difference between the two measured transmitted powers. The comparison of the measured and simulated transmission response under normal incidence of the electromagnetic wave is shown in Fig. 15. The measured -10 dB bandwidth is 12.27 GHz from 5.68 GHz to 17.95 GHz, with respect to the transmission null at a frequency of 12.83 GHz.

Due to the limitation of frequency range (1 to 18 GHz) of horn antennas used for measurements the simulated -10 dB bandwidth (12.55 GHz from 5.45 to 18 GHz) under normal incidence is compared with the measured bandwidth. The calculated percentage error between measured and simulated bandwidth is 2.25%. This error is due to the non-linear behaviour of the dielectric substrate used and fabrication errors.

Fig. 14 — Set up for experimental measurements.

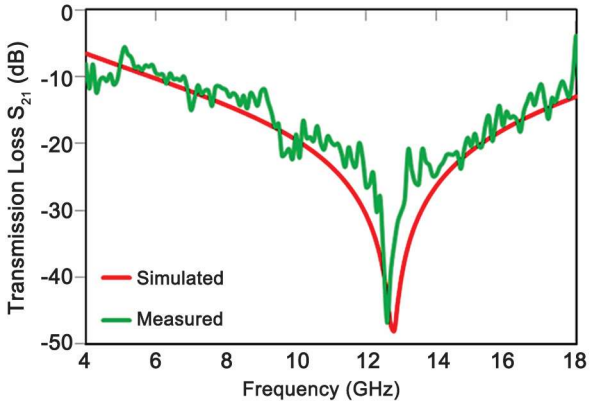


Fig. 15 — Comparison of measured and simulated transmission response.

The fabricated prototype has also been tested for different polarization angles (ϕ) from 0° to 60° in the steps of 30° of the incident wave under normal incidence. It is observed from the measured response that the proposed structure is polarization insensitive as shown in Fig. 16. Further, the fabricated structure has been tested for oblique angles of the incident wave from 0° to 60° in the steps of 30° for TE polarization as shown in Fig. 17. From the measured transmission response it is observed that the proposed FSS structure shows dual stop band as the incidence angle increases, which is similar as observed from the simulation response.

The unit cell size and the overall thickness of the proposed FSS structure have also been compared with the previously reported FSS wide stop band FSSs as depicted in Table 2. It is noticed that as compared to FSSs reported in literature[15-19] the proposed FSS provides larger bandwidth with smaller unit cell size and thickness.

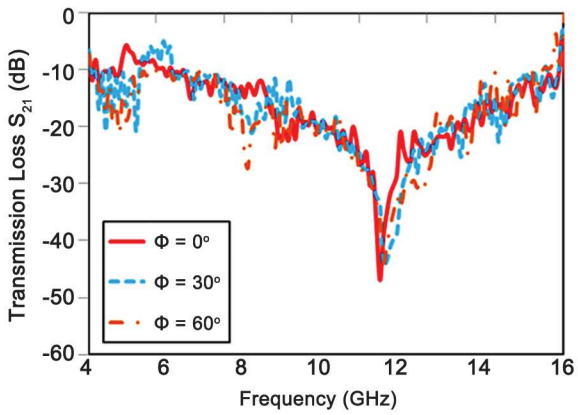


Fig. 16 — Measured response for different angles of polarization (φ) under normal incidence.

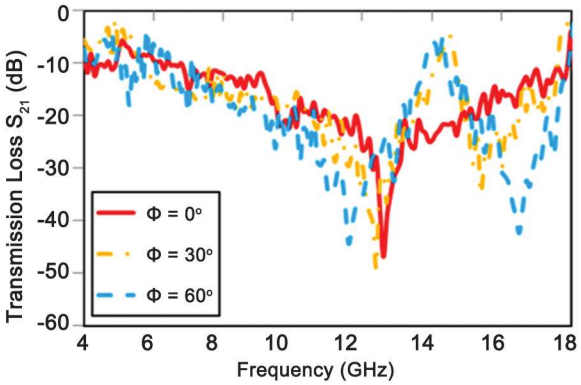


Fig. 17 — Measured response for different oblique angles of the incident wave for TE polarization.

Table 2 — Comparison of proposed FSS with the previously reported FSSs.

| Literature | -10 dB bandwidth (GHz) | Unit cell size (mm) | Thickness |
|---|---|---|---|
| Sivasamy *et al.*[12] | 4–14 (100%) | 14 ($0.47\lambda_0$) | 1.6 ($0.05\lambda_0$) |
| Chatterjee and Parui[13] | 4–7 (54%) | 11 ($0.20\lambda_0$) | 6.4 ($0.12\lambda_0$ ) |
| Kushwaha *et al.*[14] | 2.8–11 (119%) | 16 ($0.37\lambda_0$) | 1.8 ($0.04\lambda_0$) |
| Braz and Campos[15] | 8–13 (45%) | 20 ($0.70\lambda_0$) | 1.6 ($0.06\lambda_0$ ) |
| Sohail *et al.*[16] | 6.5–14 (74%) | 12 ($0.41\lambda_0$) | 3.5 ($0.11\lambda_0$) |
| Yahya *et al.*[17] | 3–12 (120%) | 8 ($0.20\lambda_0$) | 0.635 ($0.02\lambda_0$) |
| Proposed FSS | 5.45–21.41 (119%) | 7.24 ($0.32\lambda_0$) | 1.0 ($0.04\lambda_0$) |

## 6 Conclusions

In this paper a polarization insensitive frequency selective surface design is presented for wide stop band applications such as RCS reduction and minimization of electromagnetic interference and spatial filter, etc. The designed FSS consists of combination of Jerusalem cross and square loop type FSS elements to achieve wide stop band. The unit cell size of the FSS is 0.32 $\lambda_0$ and the overall thickness of the structure is 0.043 $\lambda_0$. The proposed FSS exhibits -10 dB bandwidth of 15.96 GHz from 5.45 GHz to 21.41 GHz. The equivalent circuit analysis of the individual FSS elements has also been done to get the better physical insight of the operation of the proposed FSS design. In comparison to the already reported[15-19] wide stop band FSSs the proposed FSS is compact in unit cell size, ultrathin in thickness and provides larger bandwidth. The proposed structure is polarization insensitive with its four fold symmetric design profile and experimental results are observed in agreement with simulated responses. Thus the proposed design is suitable as a band stop filter for C, X, Ku, and K-bands.

## References


1 Munk B A, *Frequency selective surfaces: Theory and design*, (John Wiley and Sons: New York), 2000.

2 Wang Z L, Hashimoto K, Shinhara & Matsumoto H, *IEEE Trans Microwave Theory Technol,* 47 (1999) 2039.

3 Joyal M A & Laurin J J, *IEEE Trans Antennas Propag*, 60 (2012) 3007.

4 Martini E, Caminita F, Nannetti M & Maci S, *IEEE Antennas Propagation Society International Symposium,* Albuquerque, NM, USA, 9-14 July 2006.

5 Agrawal V D & Imbriale W A, *IEEE Trans Antenna Propag*, 27 (1979) 466.

6 Costa F, Monorchio A & Manara G, *IEEE Antennas Propagation Society International Symposium*, Honolulu, HI, USA, 9-15 June 2007.

7 Costa F, Monorchio A & Manara G, *IEEE Trans Antennas Propag*, 58 (2010) 1551.

8 Wu T K, *Frequency selective surfaces and grid array,* (John Wiley and Sons: New York), 1995.

9 Rhoads C M, Frazier G, Richard G H, Kesler O B & Ryan D J, *Elecronically tunable optical periodic surface filters with an alterable resonant frequency,* US Patent 5,619,365A, April 8, 1997.

10 Antonopoulos C, Cahill R, Parker E A & Sturland I M, *IEEE Proc Microw Antennas Propag*, 144 (1997) 415.

11 Callaghan P, Parker E A & Langley R J, *IEEE Proc Microw. Antennas Propag*, 138 (1991) 448.

12 Sivasamy R, Moorthy B, Kanagasabai M, George J V, Lawrance L & Rajendran D B, *Int J Microw Wirel Technol,*9 (2015) 1.

13 Chatterjee A & Parui S K, *Radio Engineering,* 25 (2016) 67.

14 Kushwaha N, Kumar R, Krishna R V S & Oli T, *Prog Electromagn Res*, 46 (2014) 31.

15 Braz E C & Campos A L P S, *Microw Opt Technol Lett*, 56 (2014) 2217.

16 Sohail I, Ranga Y, Esselle K P & Hay S G, *IEEE 7th European Conference Anteenas and Propag* **,** Gothenburg, Sweden, 8-12 April 2013.

17 Yahya R, Nakamura A & Itami M, IEEE *International Symposium Antennas Propag*, Fajardo, Puerto Rico, 26 June-1 July 2016.

18 Zhang Q, You J & Liu C, *Nanotechnology and nanomaterials*, Edited by Barbillon Gregory, (Intech, Rijeka: Croatia), 2017.

19 Langley R J & Parker E A, *Electron. Lett*, 18 (1982) 294.

20 Al-Joumayly M & Behdad N, *IEEE Trans Antennas Propag*, 57 (2009) 452.

21 Costa F, Monorchio A & Manara G, *IEEE Antennas Propag Mag*, 54 (2012) 35.